

Triplication of the Photocurrent in Dye Solar Cells by Increasing the Elongation of the π -conjugation in Zn-Porphyrin Sensitizers

Eva M. Barea,^{*[a]} Rubén Caballero,^[b] Leticia López-Arroyo,^[b] Antonio Guerrero,^[a] Pilar de la Cruz,^[b] Fernando Langa,^{*[b]} and Juan Bisquert^{*[a]}

Porphyrins are promising sensitizers for dye solar cells (DSCs) but narrow absorption bands at 400–450 and 500–650 nm limit their light-harvesting properties. Increasing elongation of the π -conjugation and loss of symmetry causes broadening and a red-shift of the absorption bands, which considerably improves the performance of the DSC. Herein we use an oligothiénylenevinylene to bridge a Zn-porphyrin system and the anchoring group of the sensitizer. We separately study the performance of the two basic units: oligothiénylenevinylene and

Zn-porphyrin. The combined system provides a three-fold enhancement of the photocurrent with respect to parent dyes. This is caused by an additional strong absorption in the region 400–650 nm that leads to flat IPCE of 60%. Theoretical calculations support that the addition of the oligothiénylenevinylene unit as a linking bridge creates a charge transfer band that transforms a Zn-porphyrin dye into a push-pull type system with highly efficient charge injection properties.

1. Introduction

Dye-sensitized solar cells (DSCs) have attracted significant attention as low-cost alternatives to conventional solid-state photovoltaic devices. In these cells, a nanoporous material is filled with a thin layer of a sensitizer which can be photoexcited to ultimately provide a photocurrent.^[1] Ruthenium-based dyes have been used as the most successful sensitizers to date, yielding up to 11.3% solar-to-electric power conversion efficiencies under 1 sun illumination.^[2,3] However, these dyes lack some of the desired properties required for their large-scale production: low raw material costs and a good spectral matching with the solar radiation. Thus, there is real need for the development of inexpensive dyes with improved light absorption in the red and near-infrared region. Extended π -aromatic molecules have the potential to fulfill these two requirements.^[4–9]

Porphyrins are molecules that contain a heterocyclic macrocycle with a π -aromatic core. These do not rely on precious metals such as ruthenium and benefit from high molar extinction coefficients. Metaloporphyrins show an intense Soret band at 400–450 nm and moderate Q bands at 500–650 nm.^[10] Compared to the ruthenium complexes, these narrow bands limit the light-harvesting properties for porphyrin-based DSCs. However, it has been demonstrated that elongation of the π conjugation and loss of symmetry causes broadening and a red-shift of the absorption bands in porphyrins.^[9,11,12] Additionally, they present good photostability and high light-harvesting capabilities that favour applications in thin low-cost DSCs. Herein we describe the impact of using an oligothiénylenevinylene to bridge a Zn-porphyrin system and the anchoring group of the sensitizer. We show that this strategy increases the extended π system producing an exceptional absorption enlargement between 450 and 650 nm. This translates into a

three-fold photocurrent increase to reach a cell efficiency of $\eta = 4.77\%$.

2. Results and Discussion

A Zn-porphyrin sensitizer with extended absorption was synthesised by the structural combination of the Zn-porphyrin (**1**) and a previously reported dye containing two oligothiénylenevinylene units (**2**).^[13] The structures of these sensitizers (including terminal groups for anchoring to TiO₂ surface) are shown in Figure 1. Thus, the Zn-porphyrin-oligothiénylenevinylene (**3**) was designed having the main features of **1** and **2** linked by a styryl group. The porphyrins **1** and **3** dyes were prepared by Knoevenagel condensation of the corresponding aldehydes^[13] and cyanoacetic acid in 72% and 89% yield, respectively. The oligothiénylenevinylene dye (**2**) was prepared according to a previously described procedure.^[13] Further details of synthesis

[a] Dr. E. M. Barea, Dr. A. Guerrero, Prof. J. Bisquert
Photovoltaic and Optoelectronic Devices Group
Physics Department, Universitat Jaume I
12071 Castelló (Spain)
bisquert@fca.uji.es
E-mail: barea@fca.uji.es

[b] Dr. R. Caballero, L. López-Arroyo, Dr. P. de la Cruz, Prof. F. Langa
Instituto de Nanociencia, Nanotecnología y Materiales Moleculares
(INAMOL)
Universidad de Castilla La Mancha
Campus de la Antigua Fábrica de Armas Avda. Carlos III, s/n
45071 Toledo (Spain)
E-mail: Fernando.LPuente@uclm.es

Supporting information for this article is available on the WWW under <http://dx.doi.org/10.1002/cphc.201000958>.

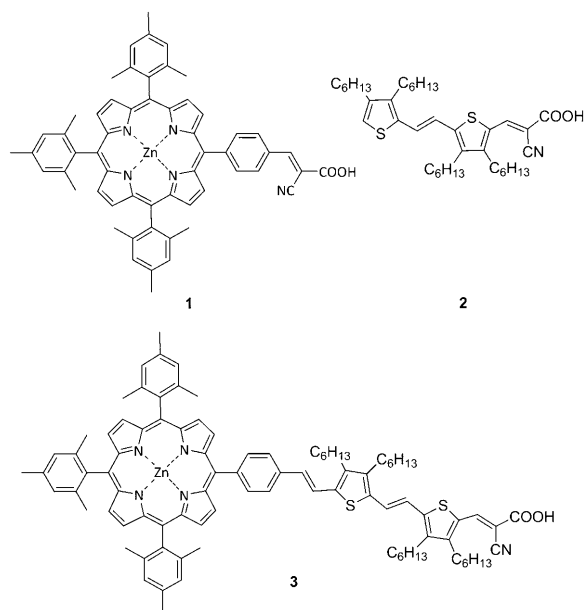


Figure 1. Structure of Zn-porphyrin dye (**1**), oligothiolenylenevinylene dye (**2**) and Zn-porphyrin-oligothiolenylenevinylene dye (**3**).

methods as well as full characterization data are given in the Supporting Information.

The electrochemical properties (Supporting Information) of the new dyes **1** and **3** were investigated by cyclic and OSW voltammetries [vs Ag/AgNO₃ in *o*-dichlorobenzene-acetonitrile (4:1) solution (0.1 mol dm⁻³ Bu₄NClO₄)] and those of **2** were previously described.^[13] Both new dyes show reversible oxidation potentials at 0.40 V and 0.73 V (**1**) and 0.33 V and 0.73 V (**3**). In addition, **3** shows a non-reversible oxidation potential at 0.53 V assigned to the oligothiolenylenevinylene bridge.^[13] The HOMO values (calculated with respect to ferrocene, HOMO: -4.8 eV) were determined as -5.01 eV for **1** and -5.03 eV for **3**. Thus, the introduction of the electroactive π bridge should favour a cascade electron transfer process increasing the lifetime of the charge separated state by slowing down the charge recombination process.

UV/Vis spectra of dyes **1** and **3** in solution of dichloromethane are shown in Figure 2. Dye **1** shows the typical absorp-

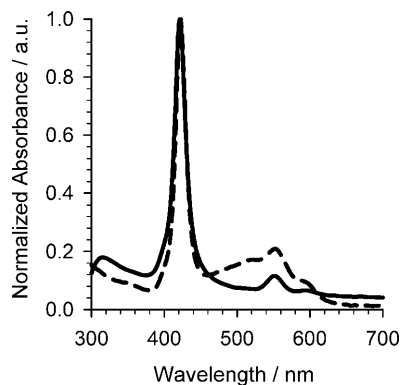


Figure 2. Normalized UV/Vis spectra in dichloromethane solution of dyes **1** (—) and **3** (----).

tion spectra of a porphyrin moiety with bands at 422 nm (log $\epsilon = 5.4$, Soret band) and 551 nm and 594 nm (log $\epsilon = 4.4$ and 4.2 respectively, Q bands). In addition to the Q band, **3** shows broader and increased intensity absorption between 430 nm and 630 nm due to presence of the oligothiolenylenevinylene π system, with a maximum at 552 nm (log $\epsilon = 4.72$).^[13]

Figure 3 shows the steady-state fluorescence spectra in dichloromethane of dye **3** (—) and the same dye containing TiO₂ attached to the carboxylic acid group (----). By excitation

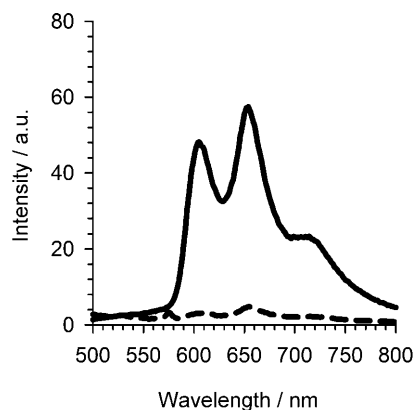


Figure 3. Emission spectra of dye **3** (dichloromethane, $\lambda_{exc} = 422$ nm) in the absence (—) and presence (----) of TiO₂.

at 422 nm (Soret band of the Zn-porphyrin) in the absence of TiO₂ the spectra shows photoluminescence of the ZnP* moiety (maxima at 606 and 650 nm). On the other hand, in the presence of TiO₂, the fluorescence intensity was significantly reduced to provide nearly quantitative quenching. This fluorescence quenching can be attributed to the photoinduced electron transfer process from Zn-porphyrin to the TiO₂ surface, favored by the efficiency of oligothiolenylenevinylene acting as a wire between donors and acceptors.^[13] Similar fluorescence effect is observed for dye **1** in the presence of TiO₂ (Supporting Information), exciting at the same wavelength (Soret band of the porphyrin). However, only partial quenching is observed for dye **2** excited at 488 nm. These results are interesting as in the operating DSC the dye **3** is attached to TiO₂ through a oligothiolenylenevinylene unit which itself does not show such good charge transfer properties for dye **2**. Thus, the porphyrin moiety is determining the charge transfer and injection properties for dye **3**.

Density functional theory (DFT) is known to be a powerful tool to elucidate the fundamental electronic processes taking place during light absorption and charge transport.^[14] Here, the geometries of the dyes **1**, **2** and **3** were optimised at the B3LYP/6-31G(*) level of theory using Gaussian 03 (see the Supporting Information for details). The optimized geometry of oligothiolenylenevinylene dye adopts a planar conformation with both the highest occupied molecular orbital (HOMO) and the lowest unoccupied molecular orbital (LUMO) delocalized along the total extent of the conjugated backbone (Figure 4). These are primarily comprised of the π framework of the thiophene,

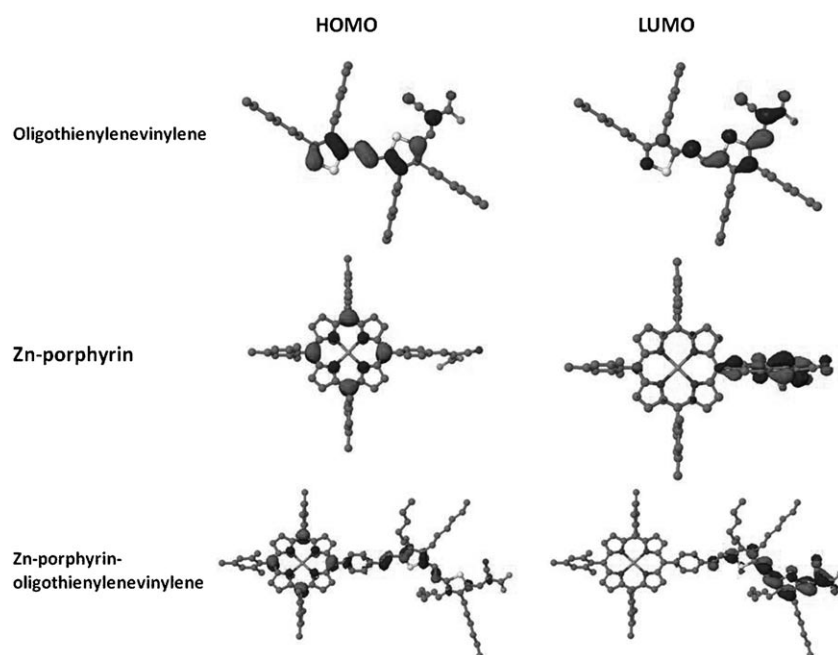


Figure 4. Optimized geometries of Zn-porphyrin (1), oligothiylenevinylene (2), and Zn-porphyrin-oligothiylenevinylene (3) dyes with HOMO (left) and LUMO (right) orbitals. The surfaces were generated with an isovalue at 0.035 and hydrogen atoms are omitted for clarity.

vinylidene, cyano and anchoring groups. Alternatively, Zn-porphyrin presents a conformation with a planar porphyrin moiety with three perpendicular trimethylbenzenes and one aryl ring linked with the porphyrin. Whilst the HOMO is localized in the porphyrin ring, the LUMO is mainly delocalized in the region of the anchoring group with a small contribution in the porphyrin ring. Finally, the optimized geometry of dye **3** is similar to the Zn-porphyrin **1** around the porphyrin unit and as planar as oligothiylenevinylene dye in its analogous part. The HOMO is delocalized in the porphyrin and thiophene vinylidene groups with a small contribution of the phenyl and anchoring group. On the other hand, the LUMO is well localized in thiophene vinylidene and anchoring groups with no contribution of the porphyrin moiety. In this last dye, the total split of π and π^* orbitals in the porphyrin core enhances charge transfer and charge separation processes. Calculated energy values for HOMO and LUMO and E_g (LUMO–HOMO) are shown in Table 1. These results clearly reveal a decrease in the E_g from the parent dyes to the Zn-porphyrin-oligothiylenevinylene that explains the red-shift in the absorption band.

	HOMO [eV]	LUMO [eV]	$E_g^{[a]}$ [eV]
Zn-porphyrin (1)	–5.23	–2.62	2.61
Oligothiylenevinylene (2)	–5.29	–2.62	2.67
Zn-porphyrin-oligothiylenevinylene (3)	–5.01	–2.83	2.18

[a] E_g = LUMO–HOMO

Figure 5 shows the film absorption spectra of the three dyes under study and N719 as reference dye. All the spectra were taken under the same conditions (0.3 mM dye solution, 2 h absorption time). Both parent dyes **1** and **2** show a band with λ_{\max} at approximately 420 nm. Additionally, the Zn-porphyrin dye confirms the typical Q band at 580 nm. The addition of two thiylenevinylene units to the Zn-porphyrin provides a new absorption area between 450 and 650 nm for the sensitizer **3**, due to the elongation of the π -conjugated system that splits the π and π^* levels in the porphyrin gap between the HOMO and the LUMO. Thus, this structural change leads to broadening and red shift of the absorption bands together with an increased in-

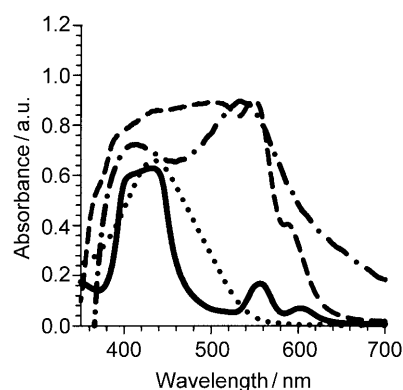


Figure 5. UV/Vis spectra for Zn-porphyrin (1, —), oligothiylenevinylene (2,), Zn-porphyrin-oligothiylenevinylene (3, ----) and N719 dyes (– · – ·) attached to transparent TiO_2 films

tensity, especially that of the Q bands relative to the Soret band.

By the integration of the absorption spectra of Figure 5 with the solar spectrum, it is possible to calculate the maximum current that we can obtain from each dye, without any contribution like the recombination or regeneration process that could take place during the DSC's performance. For the parent dyes **1** and **2**, the maximum current that we can get is 11.8 and 11 mAcm^{-2} respectively, and for the new dye **3** the maximum current is 18.2 mAcm^{-2} , which will translate to a higher overall conversion efficiency due to a push–pull-type system generated by the addition of the oligothiylenevinylene unit added to dye **1**. In the case of N719 dye, the current that we can get is low due to experimental conditions used for mea-

sured the UV/Vis spectra and that is reflected in the overall conversion efficiency of the N719 DSC.

From that calculation it is clearly observed that both absorption and injection contribute to the incident photon-to-current efficiencies (IPCE) reported in Figure 6. The addition of the oli-

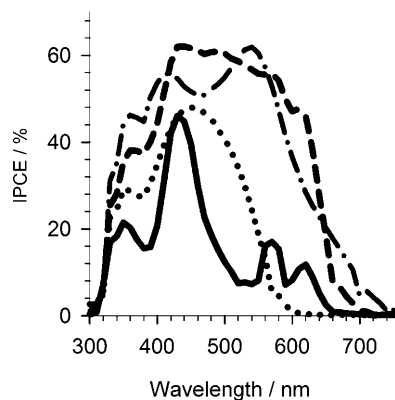


Figure 6. Incident photon-to-current efficiencies (IPCE) for Zn-porphyrin (1, —), oligothiophenevinylene (2, ·····), Zn-porphyrin-oligothiophenevinylene (3, - - - -) and N719 dyes (- · - · -).

gothiophenevinylene unit as a linking bridge through a styryl group for dye 3 transforms a Zn-porphyrin dye into a push-pull type system. Thus, the enormous gain in the absorption of the film between 450 and 600 nm observed for Zn-porphyrin-oligothiophenevinylene is also reflected in the IPCE results. This leads to an IPCE of 60% for Zn-porphyrin-oligothiophenevinylene that remains flat between 400 and 650 nm. Finally, it is important to note that IPCE results for dye 3 are similar to those obtained for a DSC sensitized with standard N719 dye fabricated under the same conditions.

The performance of DSC based on Zn-porphyrins (1 and 3), oligothiophenevinylene (2) and N719 under 1 sun illumination, is shown in Table 2 and Figure 7. It is important to note that

Table 2. Performance of the DSC devices based on the different sensitizers at 1 sun.				
Sensitizer Molecule	$V_{oc}^{[a]}$ [V]	$j_{sc}^{[b]}$ [mA cm^{-2}]	FF ^[c]	$\eta^{[d]}$ [%]
Zn-porphyrin (1)	0.52	3.6	0.58	1.10
Oligothiophenevinylene (2)	0.53	5.0	0.64	1.74
Zn-porphyrin-oligothiophenevinylene (3)	0.62	15.6	0.49	4.77
N719	0.67	11.1	0.57	4.27

[a] V_{oc} is open circuit potential, [b] j_{sc} is the short circuit current, [c] FF is the fill factor and [d] η is the conversion efficiency at 1 sun.

results obtained for all dyes have been obtained using relatively thin layers of nanoporous TiO_2 (6 μm). Lower than previously reported efficiencies obtained for N719 are expected as a result of the fabrication conditions: (1) relatively short time deep in dye solution (2 h) combined with low absorption coefficient of the Ruthenium sensitizer and (2) the electrolyte com-

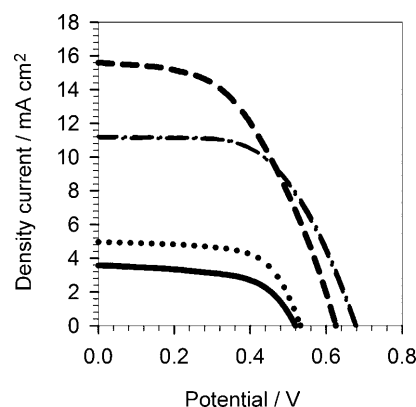


Figure 7. j - V curves of DSCs sensitized with Zn-porphyrin (1, —), oligothiophenevinylene (2, ·····), Zn-porphyrin-oligothiophenevinylene (3, - - - -) and N719 dyes (- · - · -) under standard conditions (100 mW cm^{-2} , AM1.5).

position without ionic liquid. Herein, both Zn-porphyrin 1 and oligothiophenevinylene 2, provide a modest overall conversion efficiency that remains below 2%. Compared with the parent dyes, the Zn-porphyrin-oligothiophenevinylene presents an increment in the photocurrent of around 300% and a 100 mV higher open-circuit voltage, producing a large increment of the overall solar cell performance to 4.77%.

3. Conclusions

In conclusion, we showed that the strategy based on elongation of the π conjugation and loss of symmetry in porphyrins produces an enhancement in both the short circuit photocurrent and open-circuit potential, due to an important increase in the light absorption and improved charge injection in the DSC. Thus, the performance of both Zn-porphyrin and oligothiophenevinylene dyes has been improved significantly from 1.10% and 1.74%, respectively, by using a combination of their structures to $\eta=4.77\%$, obtaining similar efficiency to N719 dye under the same DSC fabrication conditions. PL measurements prove that good electron transfer takes place for the improved porphyrin (3) system that enables good electron injection into the TiO_2 . Alternatively, theoretical study by DFT supports an enhancement in the light absorption. This improvement is obtained by the increase in the conjugation of the π system that reduces the E_g red-shifting the absorption and gives rise to a charge transfer state by completely removing the participation of the porphyrin system in the LUMO of the molecule. Both of these aspects contribute to an increased IPCE and higher overall energy conversion efficiency.

Experimental Section

Dye solar cells (DSC) were prepared using TiO_2 nanocrystalline paste (50 nm particle size from Dyesol). The TiO_2 layers were deposited with the Doctor Blading technique on transparent conducting oxide (TCO) glass (Pilkington TEC15, $\sim 15 \Omega \square^{-1}$ resistance). The resulting photoelectrodes of 6 μm thickness, were sintered at 450°C and then immersed in 0.04 M TiCl_4 solution for 30 min at

70 °C followed by calcination at 450 °C for 30 min to obtain good electrical contact between the nanoparticles. When the temperature decreased to 40 °C all the electrodes were immersed into dye solution (0.3 mm in dichloromethane and 0.3 mm acetonitrile/tert-butanol for N719) for 2 h. After the adsorption of the dye, the electrodes were rinsed with the same solvent. The solar cells were assembled with counter electrode (thermally platinized TCO) using a thermoplastic frame (Surlyn 25 µm thick). Redox electrolyte [0.5 M LiI (99,9%), 0.05 M I₂ (99,9%) and 0.5 M 4-tertbutylpyridine in 3-methoxypropionitrile] was introduced through a hole drilled in the counter electrode that was sealed afterwards. Prepared solar cells (0.4 cm² size, masking solar cell to 0.25 cm²) were characterized by thin-film absorption measurements, current–voltage characteristics and incident photon to current efficiency (IPCE). UV/Vis data was obtained using a Cary 300 Bio Spectrophotometer with the adequate setup for thin-film analysis. Photocurrent and voltage were measured using a solar simulator equipped with a 1000 W ozone-free Xenon lamp and AM 1.5 G filter (Oriel), were the light intensity was adjusted with an NREL-calibrated Si solar cell with a KG-5 filter to 1 sunlight intensity (100 mW cm⁻²) and a 250 W Xenon arc lamp (Oriel) served as a light source for IPCE.

Acknowledgements

We thank financial support from Ministerio de Ciencia e Innovación under Projects HOPE CSD2007–00007 and CTQ2007–63363/PPQ, JJCC de Castilla-La Mancha (Project PCI08–038), Project ORION FP7-NMP-2008-LARGE-2 and Generalitat Valenciana under Project PROMETEO/2009/058.

Keywords: dye-sensitized solar cells • dyes/pigments • porphyrinoids • UV/Vis spectroscopy • zinc

- [1] B. O'Regan, M. Grätzel, *Nature* **1991**, 353, 737–740.
- [2] M. K. Nazeeruddin, F. De Angelis, S. Fantacci, A. Selloni, G. Viscardi, P. Liska, S. Ito, T. Bessho, M. Grätzel, *J. Am. Chem. Soc.* **2005**, 127, 16835–16847.
- [3] F. Gao, Y. Wang, D. Shi, J. Zhang, M. Wang, X. Jing, R. Humphry-Baker, P. Wang, S. M. Zakeeruddin, M. Grätzel, *J. Am. Chem. Soc.* **2008**, 130, 10720–10728.
- [4] S. Hayashi, Y. Matsubara, S. Eu, H. Hayashi, T. Umeyama, Y. Matano, H. Imahori, *Chem. Lett.* **2008**, 37, 846–847.
- [5] S. Hayashi, M. Tanaka, H. Hayashi, S. Eu, T. Umeyama, Y. Matano, Y. Araki, H. Imahori, *J. Phys. Chem. C* **2008**, 112, 15576–15585.
- [6] Q. Wang, W. M. Campbell, E. E. Bonfantani, K. W. Jolley, D. L. Officer, P. J. Walsh, K. Gordon, R. Humphry-Baker, M. K. Nazeeruddin, M. Grätzel, *J. Phys. Chem. B* **2005**, 109, 15397–15409.
- [7] W. M. Campbell, K. W. Jolley, P. Wagner, K. Wagner, P. J. Walsh, K. C. Gordon, S.-M. Lukas, M. K. Nazeeruddin, Q. Wang, M. Grätzel, D. L. Officer, *J. Phys. Chem. C* **2007**, 111, 11760–11762.
- [8] Y. Tachibana, S. A. Haque, I. P. Mercer, J. R. Durrant, D. R. Klug, *J. Phys. Chem. B* **2000**, 104, 1198–1205.
- [9] H.-P. Lu, C.-Y. Tsai, W.-N. Yen, C.-P. Hsieh, C.-W. Lee, C.-Y. Yeh, E. Wei-Guang Diao, *J. Phys. Chem. C* **2009**, 113, 20990–20997.
- [10] H. Imahori, T. Umeyama, S. Ito, *Acc. Chem. Res.* **2009**, 42, 1809–1818.
- [11] C. Y. Lee, J. T. Hupp, *Langmuir* **2010**, 26, 3760–3765.
- [12] S.-L. Wu, H.-P. Lu, H.-T. Yu, S.-H. Chuang, C.-L. Chiu, C.-W. Lee, E. Diao, C.-Y. Yeh, *Energy Environ. Sci.* **2010**, 3, 949–955.
- [13] E. M. Barea, R. Caballero, F. Fabregat, -Santiago, P. de La Cruz, F. Langa, J. Bisquert, *ChemPhysChem* **2010**, 11, 245.
- [14] P. Qin, M. Linder, T. Brinck, G. Boschloo, A. Hagfeldt, L. Sun, *Adv. Mater.* **2009**, 21, 2993–2996.

Received: November 17, 2010

Revised: January 28, 2011

Published online on March 4, 2011